Electronic Supplementary Information

Highly Selective Photo-hydroxylation of Phenol Using Ultrathin NiFe-layered Double Hydroxide Nanosheets under Visible-light up to 550 nm

Jikang Wang,[a] Yanqi Xu,[ac] Jiaxin Li,[a] Xiaodong Ma,[a] Si-Min Xu, [a] Rui Gao,[b] Yufei Zhao *[a] and Yu-Fei Song *[a]

[a] State Key Laboratory of Chemical Resource Engineering, Beijing University of Chemical Technology, 100029 Beijing, P. R. China

[b] School of Chemistry and Chemical Engineering, Inner Mongolia University, 010021 Hohhot, P. R. China

[c]College of Materials Science and Engineering, Guilin University of Technology, Guilin 541004, China

* Corresponding author

Email: songyf@mail.buct.edu.cn, zhaoyufei@mail.buct.edu.cn. Tel/Fax: +86 10 64431832

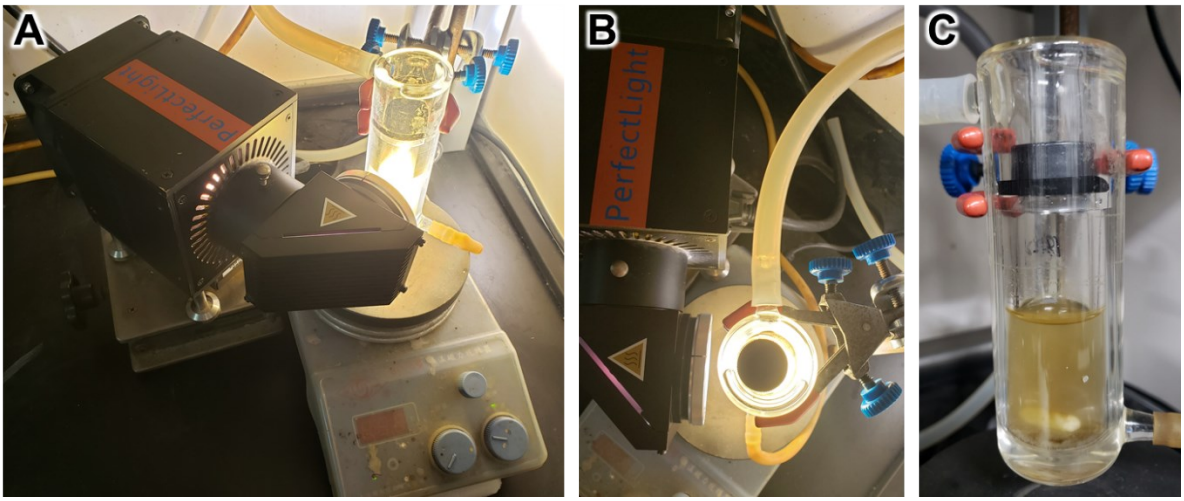

Figure S1. The reaction devices, including reaction tube, condensing tube, magnetic stirrer and 300 W Xenon lamp source (PLS-SXE300D of Beijing Perfectlight Technology Co., Ltd).

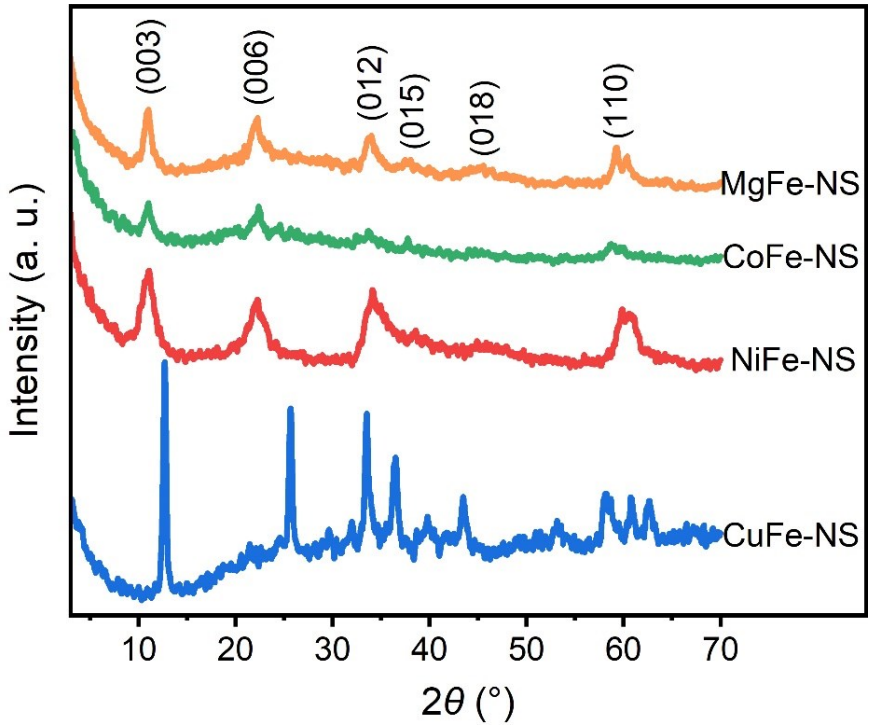

Figure S2. XRD patterns for $M^{II}Fe$-LDHs nanosheets (M= Mg, Co, Ni, Cu), respectively.

The XRD pattern of CuFe-NS showed a series of unique diffraction peaks consistent with the literature reports,[1-4] proving that it was indeed CuFe-LDH material.

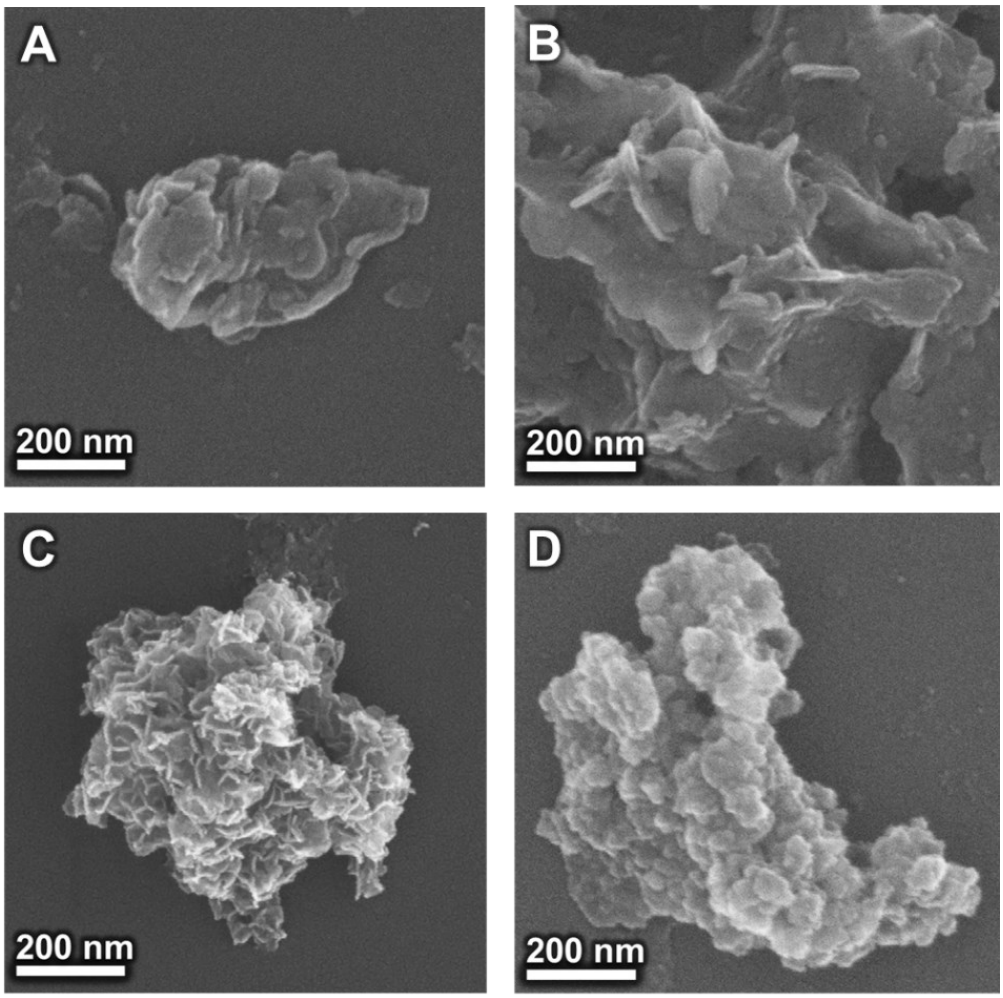

Figure S3. SEM images for (A) MgFe-NS, (B) CoFe-NS, (C) NiFe-NS, and (D) CuFe-NS, respectively.

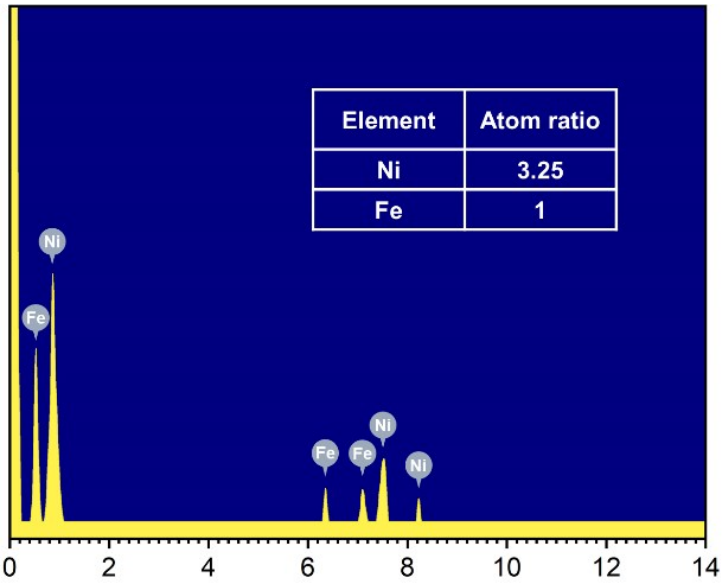

Figure S4. Energy-dispersive X-ray spectroscopy of NiFe-NS.

Table S1. The mass of the starting materials and the products for the synthesis of $M^{II}Fe$-NS.

	The mass of starting materials (g)				The mass of products (g)
	Divalent metallic nitrate	$Fe(NO_3)_3 \cdot 9H_2O$	NaOH	$NaNO_3$	
MgFe-NS	8.21	4.61	2.73	1.81	~1.7
CoFe-NS	9.31	4.61	2.73	1.81	~2.4
NiFe-NS	9.31	4.61	2.73	1.81	~2.8
CuFe-NS	7.73	4.61	2.73	1.81	~2.1

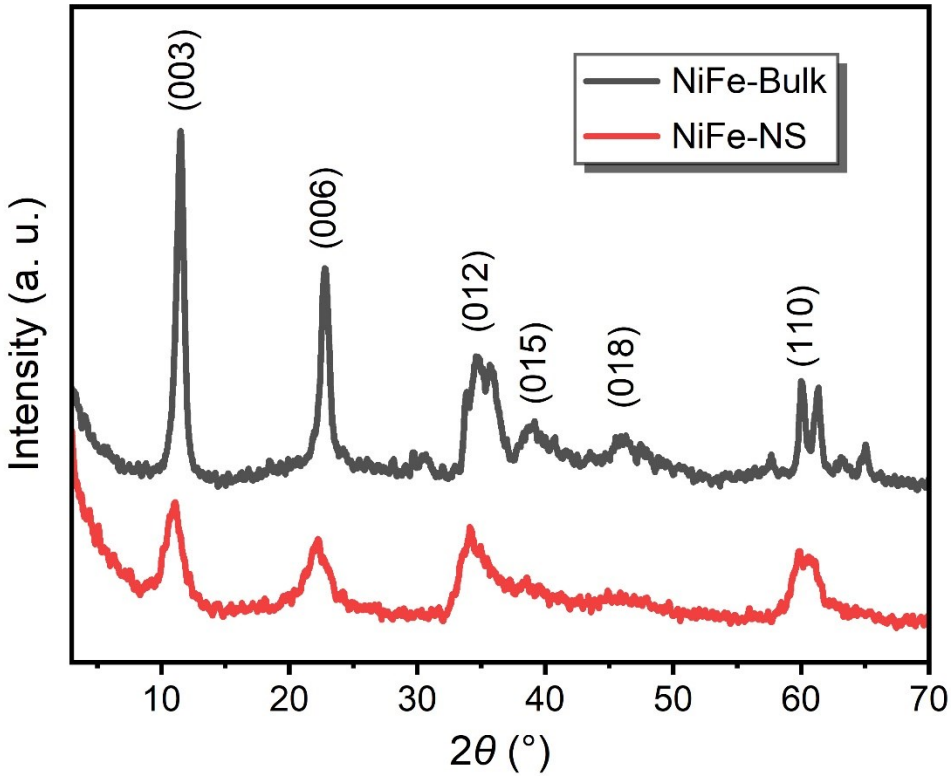

Figure S5. XRD patterns for NiFe-NS and NiFe-Bulk, respectively.

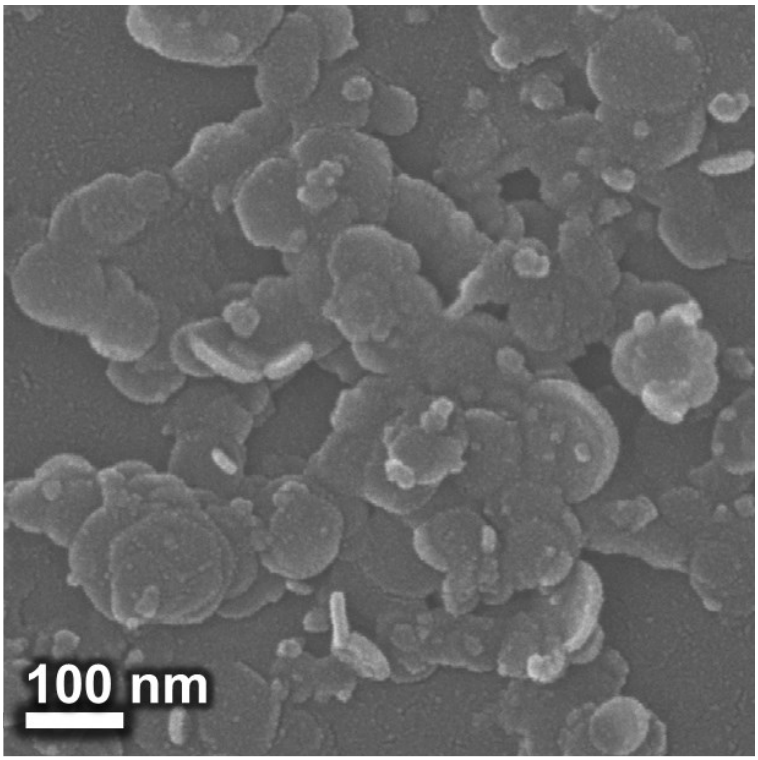

Figure S6. SEM image for NiFe-Bulk.

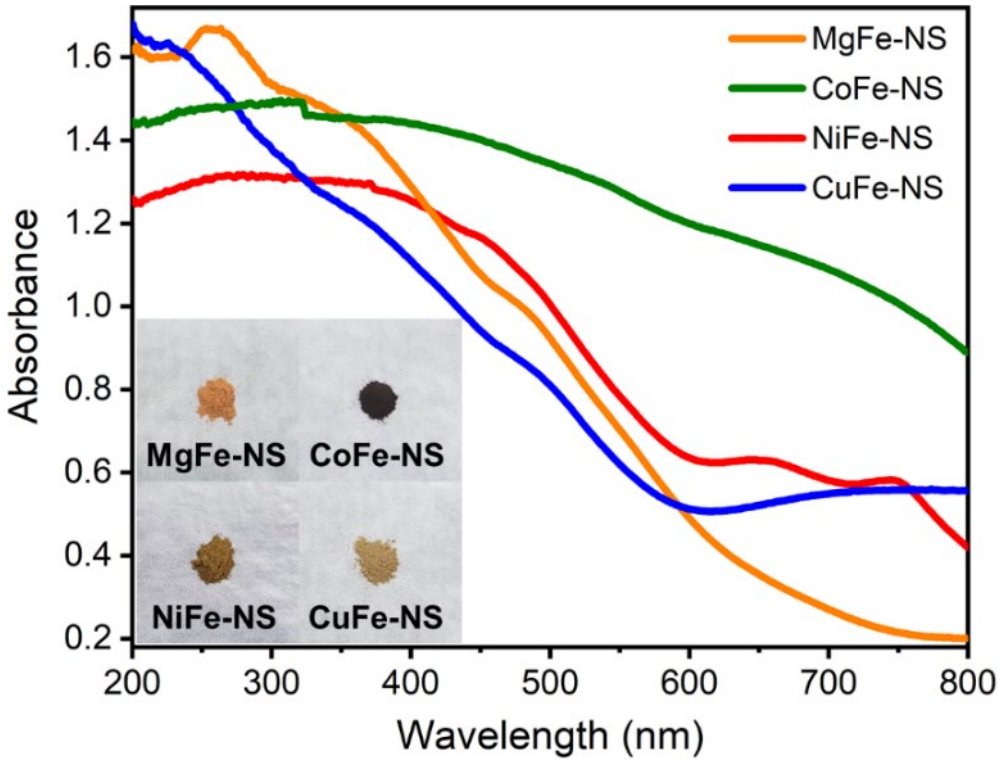

Figure S7. UV–vis diffuse reflectance spectra over MgFe-NS, CoFe-NS, NiFe-NS, and CuFe-NS, respectively (the inset shows the digital images of the above LDHs).

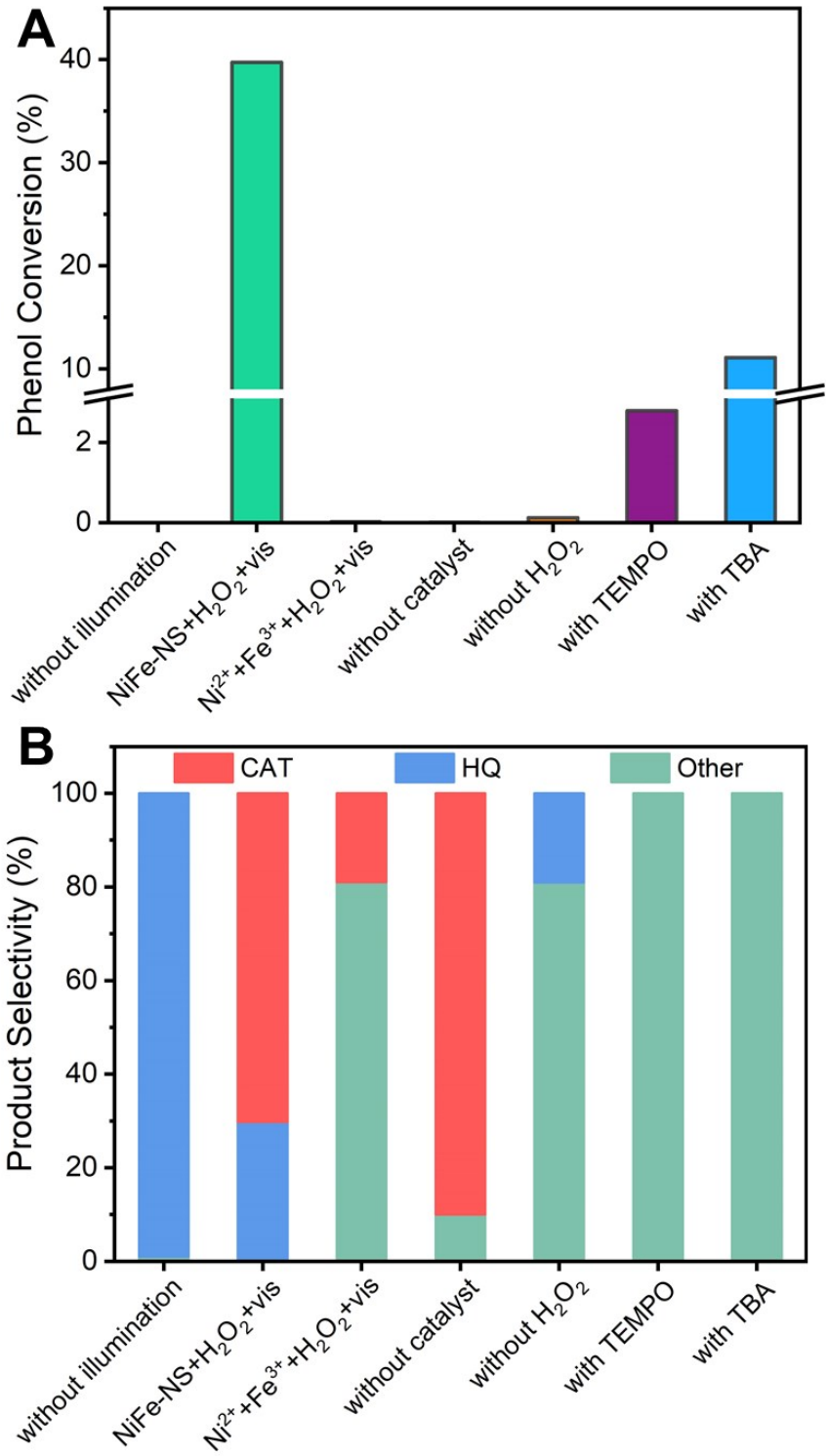

Figure S8. (A) Phenol conversion and (B) product selectivity of control experiment under different conditions.

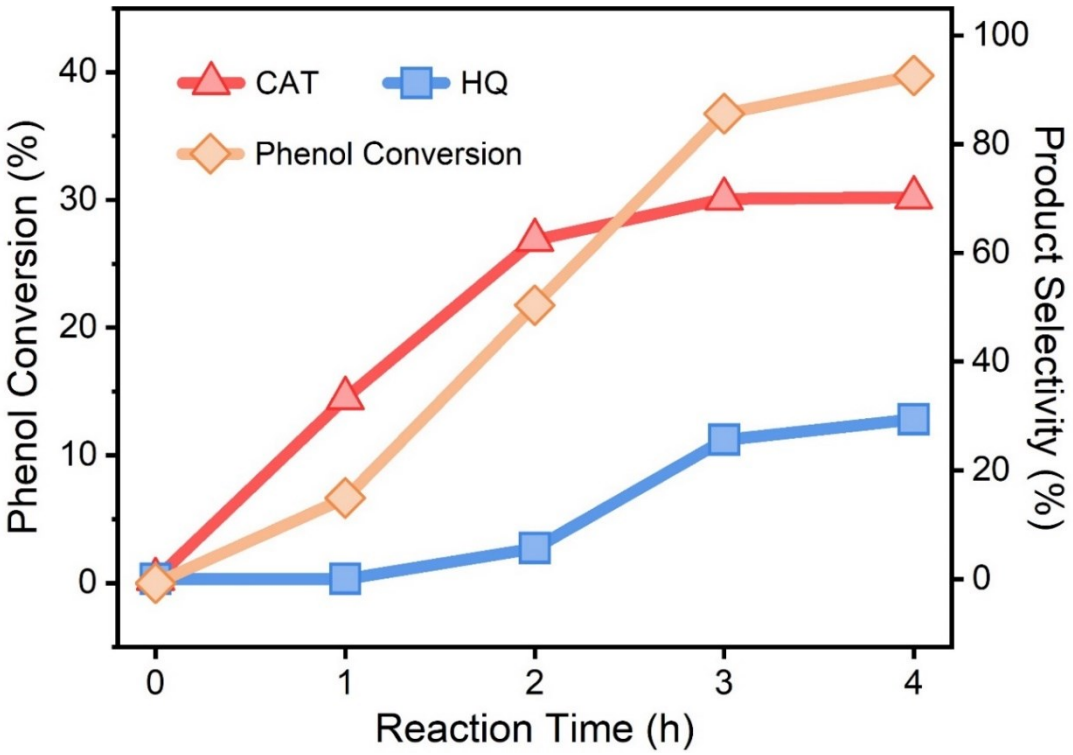

Figure S9. Time course of phenol conversion and product selectivity over NiFe-NS.

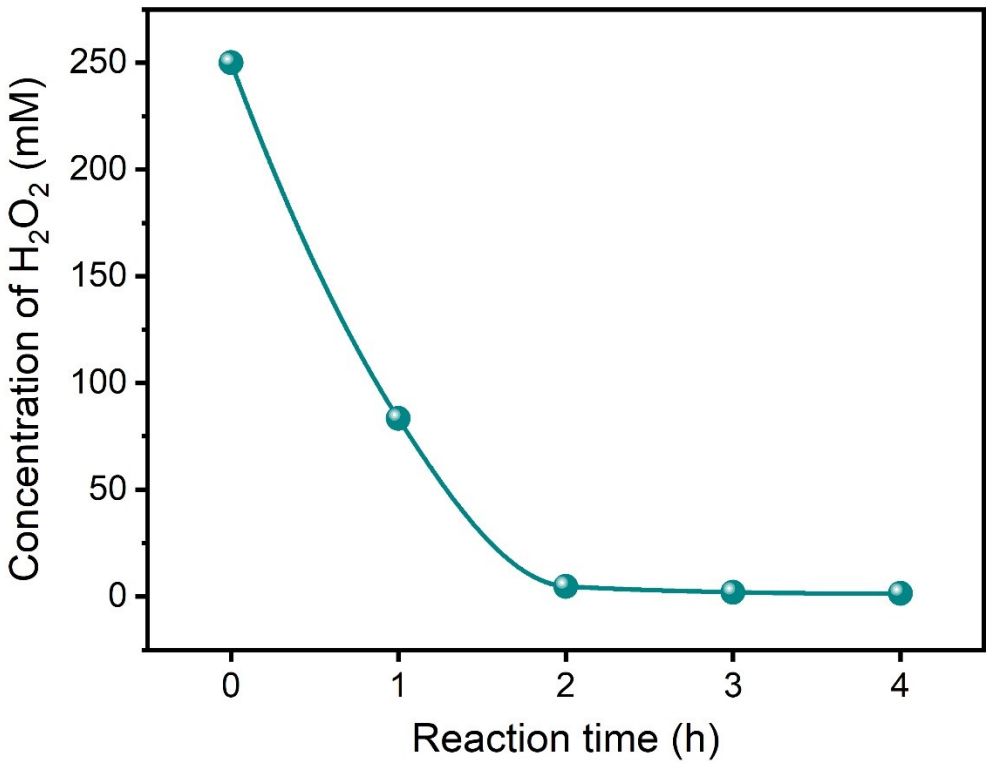

Figure S10. Time course of H_2O_2 concentration during the reaction.

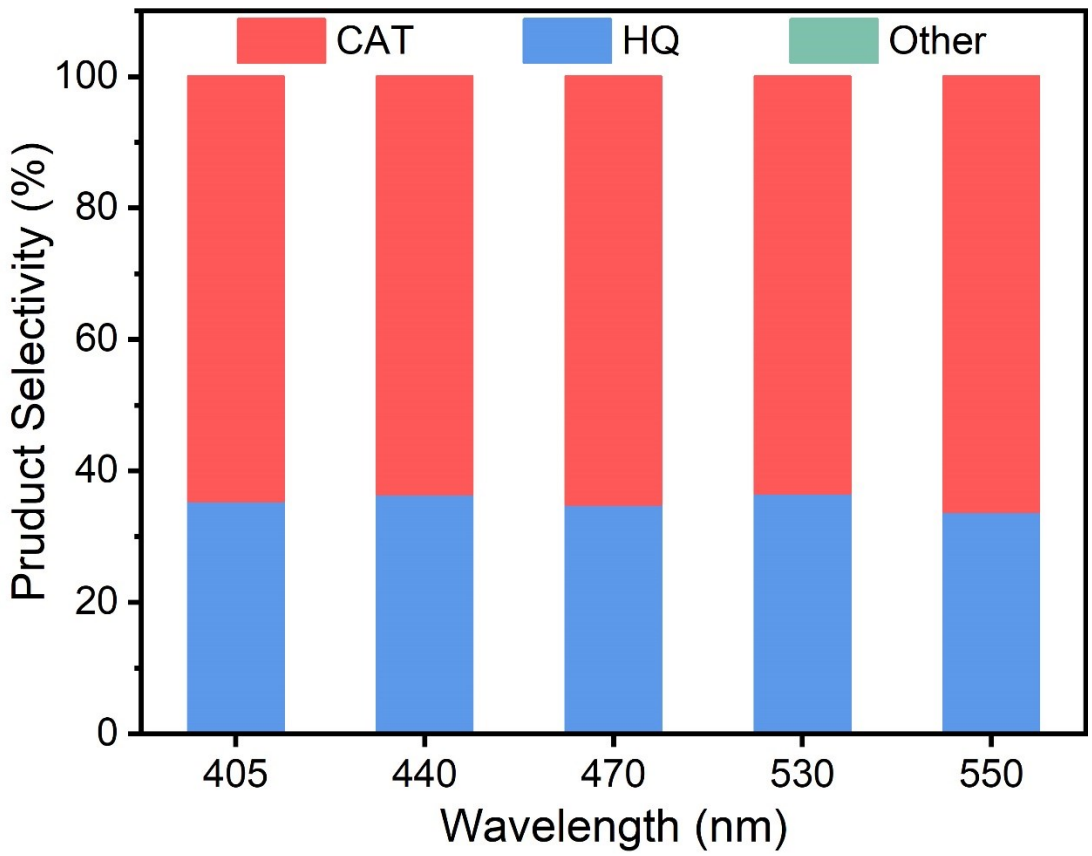

Figure S11. Product selectivity over NiFe-NS under monochromatic excitation at 405, 440, 470, 530, and 550 nm. The catalyst has no catalytic activity under irradiation above 600 nm.

Table S2. Comparison of phenol hydroxylation performance for various catalysts in previous literature and this work.

Catalyst	Phenol Conc. (mM)	H_2O_2 Conc. (mM)	Solvent	Temp. or light source	Reaction Time (h)	Phenol Conv. (%)	DHB Sel. (%)	Ref.
Al-Free Mn-β	644	322	H_2O	80°C	6	35.2	97.8	ACS Appl. Mater. Interfaces 7 (2015) 2424-2432 [5]
Fe/WAC/6.94	500	500	H_2O	40°C	0.7	51.7	80.3	Catal. Sci. Technol. 5 (2015) 2486-2495 [6]
MFS-2	333	333	H_2O	70°C	3	52	72	J. Colloid Interface Sci. 380 (2012) 16-24 [7]
Fe-SPC-2	333	333	H_2O	50°C	3	46.2	70.6	Appl. Surf. Sci. 285 (2013) 721-726 [8]
RH-10Fe	2000	4000	H_2O	70°C	2	95.2	100	Chem. Eng. J. 165 (2010) 658-667 [9]
Fe/KL	1000	2000	H_2O	70°C	0.5	93.4	100	Chem. Eng. J. 214 (2013) 63-67 [10]
FeVCN 55	1667	4167	ACN	60°C	4	40.5	9.6	Appl. Catal. B Environ. 218 (2017) 621-636 [11]
4Cu-4PAAm-3GO-ALG	353	647	H_2O	70°C	2	78.5	95.9	Catal. Commun. 101 (2017) 116-119 [12]
Fe-Al-silicate	265	485	H_2O, ACN	365 nm	4	64.9	95	Catal. Commun. 12 (2011) 1022-1026 [13]
C. I. Pigment Green 8	171	243	H_2O, ACN	365 nm	4	87. 8	73.3	Curr. Org. Chem. 16 (2012) 3002-3007 [14]
NiFe-NS	**250**	**750**	**H_2O**	**25°C, 550 nm**	**4**	**69.7**	**99.7**	**This work**
NiFe-NS	**250**	**250**	**H_2O**	**25°C, vis**	**4**	**39.7**	**99.6**	**This work**
NiFe-NS	**250**	**250**	**H_2O**	**25°C, 460 nm LED**	**4**	**28.4**	**99.7**	**This work**

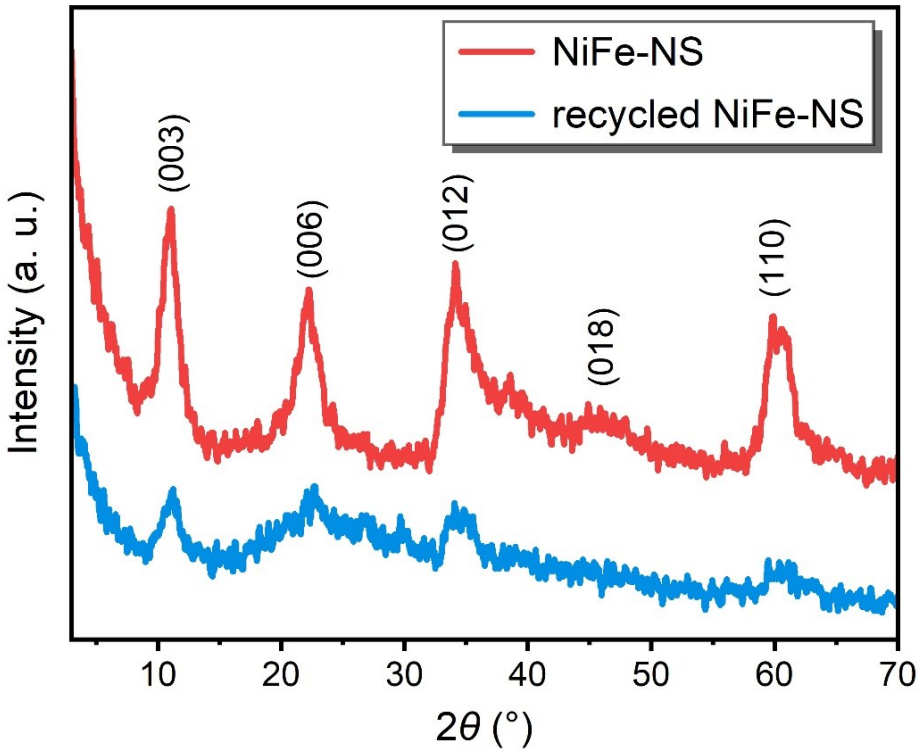

Figure S12. XRD patterns for fresh NiFe-NS and recycled NiFe-NS.

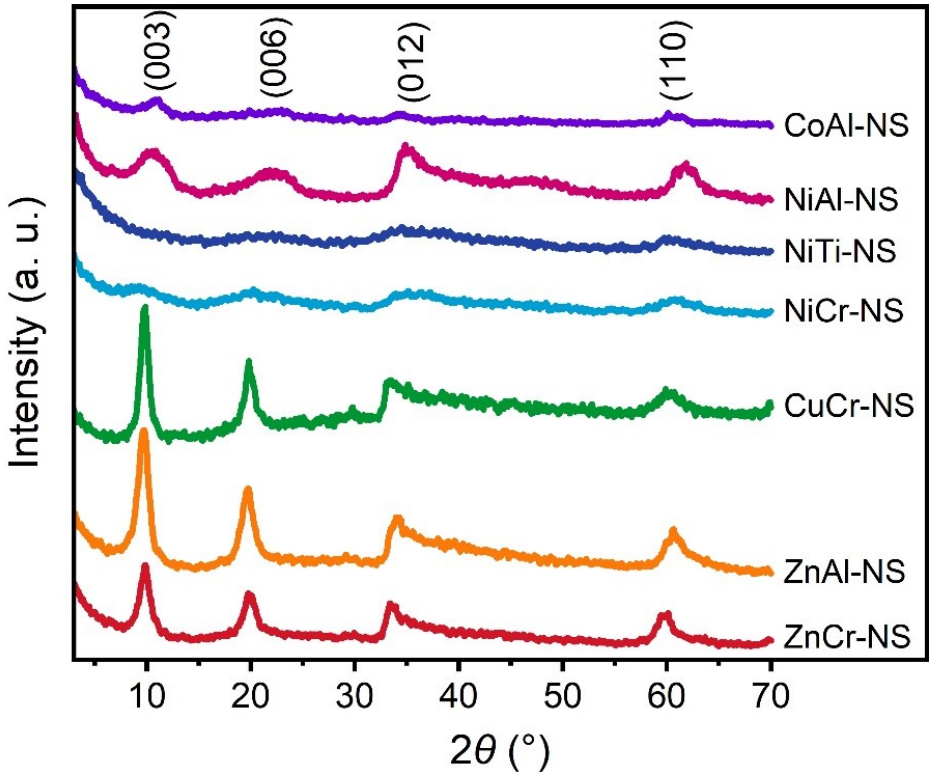

Figure S13. XRD patterns for different LDHs nanosheets.

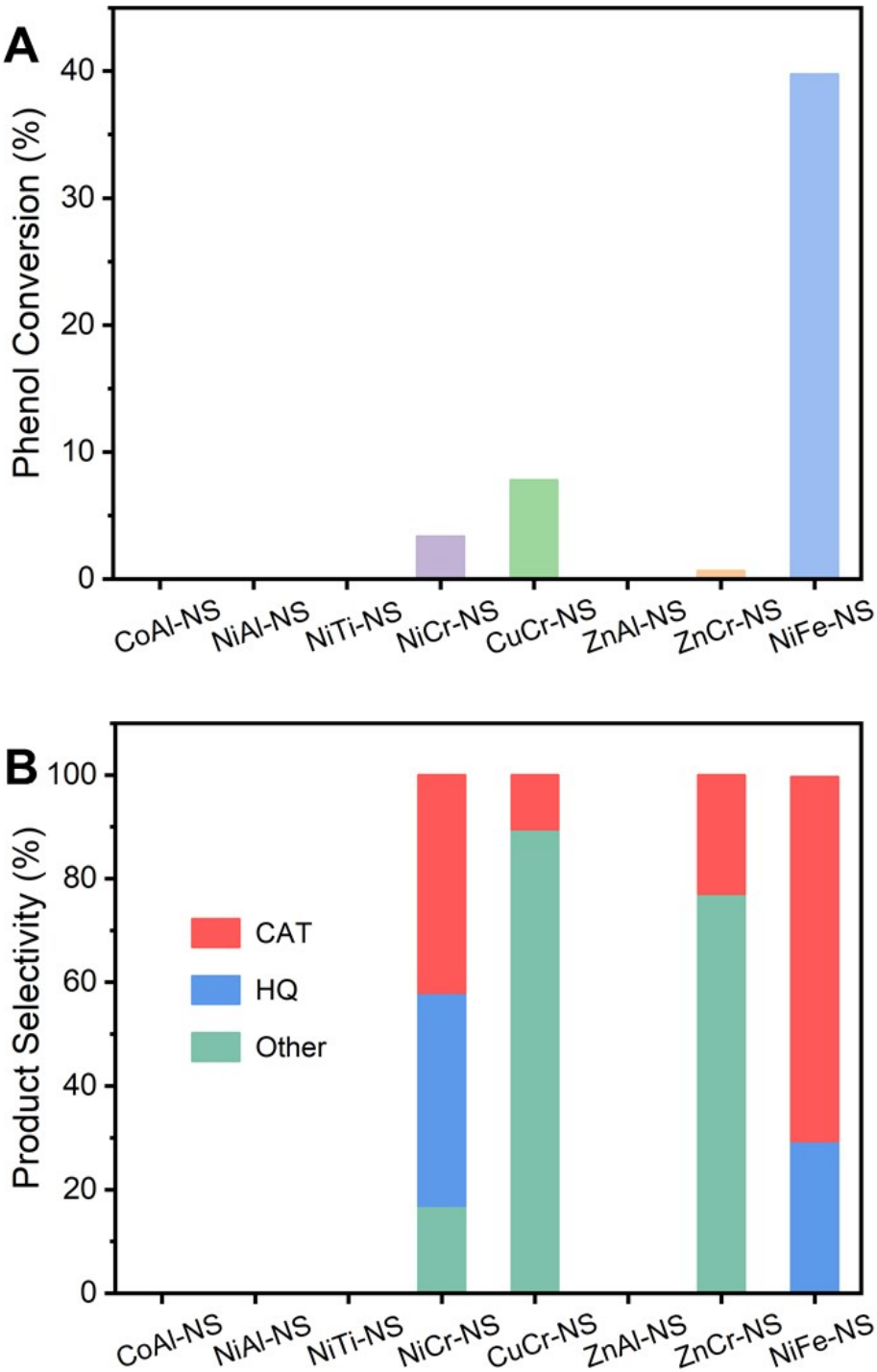

Figure S14. (A) Phenol conversion and (B) product selectivity of different LDHs under visible-light illumination.

Table S3. Local structure parameters around Ni estimated by EXAFS analysis.

Sample	Shell	*N*	*R* [Å]	σ^2 [10^{-3} Å^2]	*R-factor* [10^{-3}]
NiFe-Bulk	Ni-O	6.0	2.05	6.4	7.0
	Ni-Ni/Fe	6.0	3.10	7.2	
NiFe-NS	Ni-O	5.3	2.05	6.6	6.1
	Ni-Ni/Fe	5.4	3.10	7.5	

[a] *N* = coordination number; [b] *R* = distance between absorber and backscatter atoms; [c] σ^2= Debye-Waller factor

Table S4. Local structure parameters around Fe estimated by EXAFS analysis.

Sample	Shell	*N*	*R* [Å]	σ^2 [10^{-3} Å^2]	*R-factor* [10^{-3}]
NiFe-Bulk	Fe-O	6.0	1.99	5.7	7.7
	Fe-Ni	6.0	3.13	7.3	
NiFe-NS	Fe-O	5.8	2.00	6.1	3.2
	Fe-Ni	5.6	3.12	8.0	

[a] *N* = coordination number; [b] *R* = distance between absorber and backscatter atoms; [c] σ^2= Debye-Waller factor

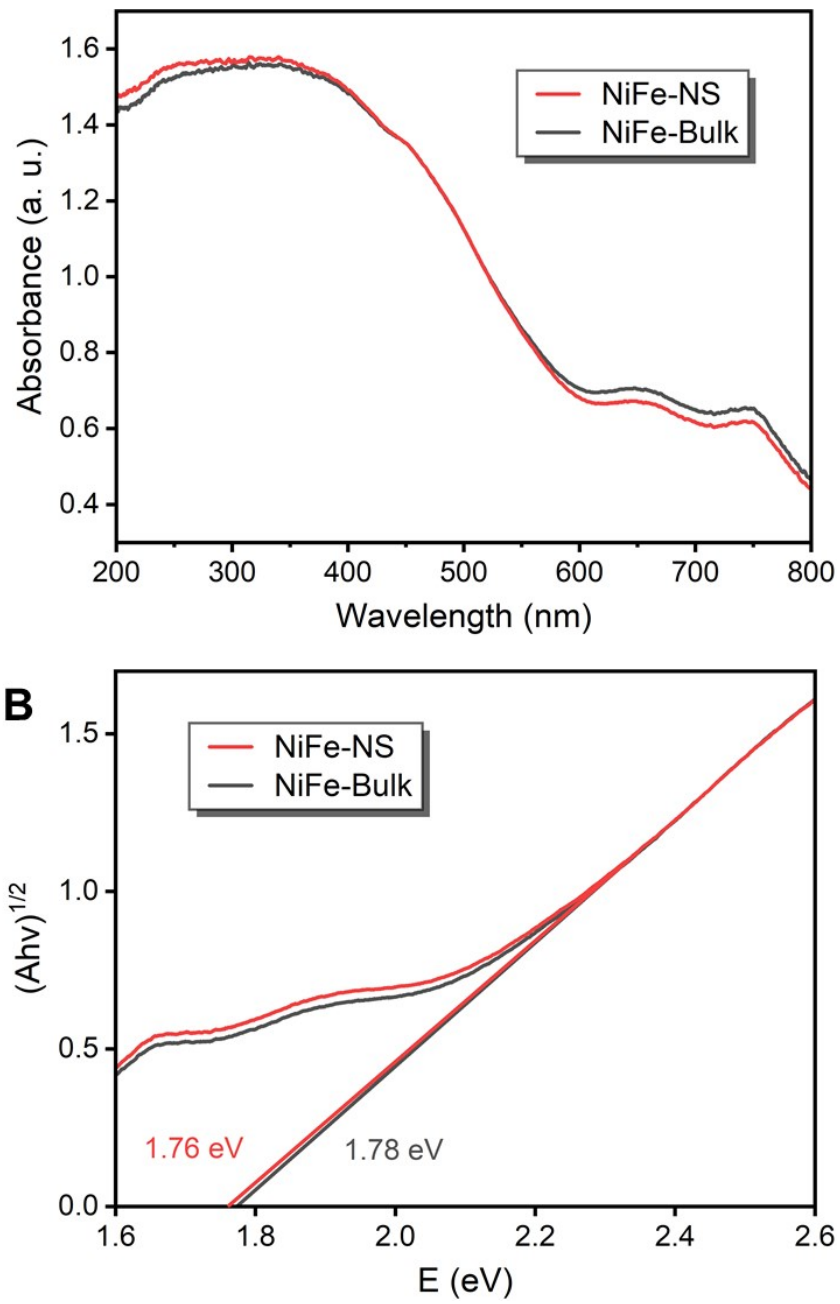

Figure S15. (A) UV-vis diffuse reflectance spectra and (B) Tauc plots of NiFe-NS and NiFe-Bulk.

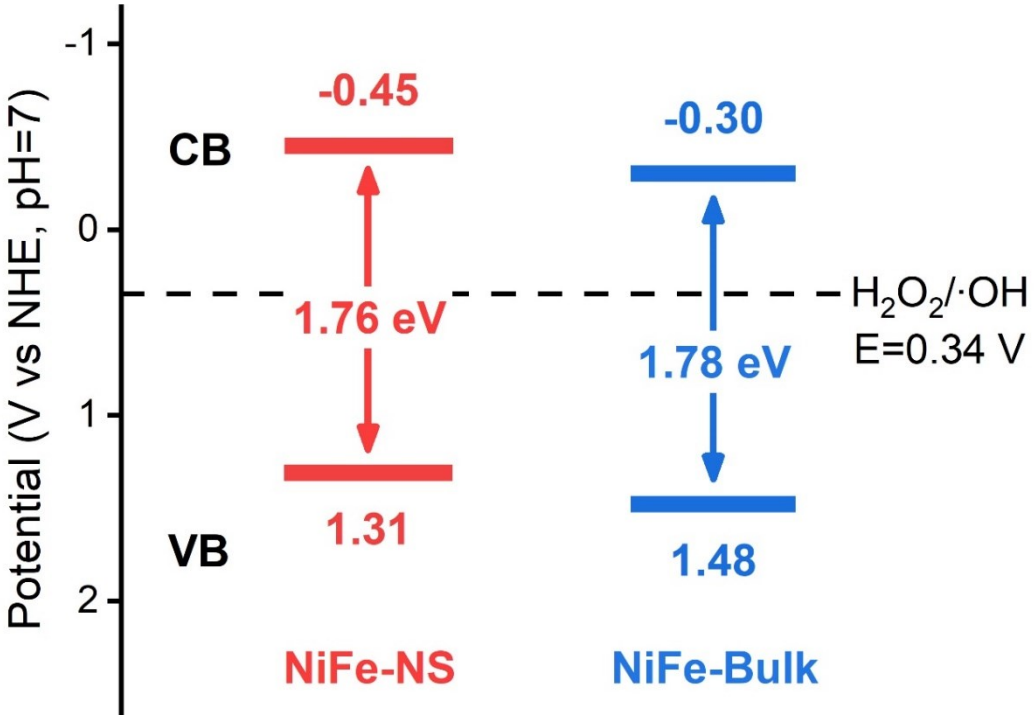

Figure S16. Schematic band diagrams of NiFe-NS and NiFe-Bulk.

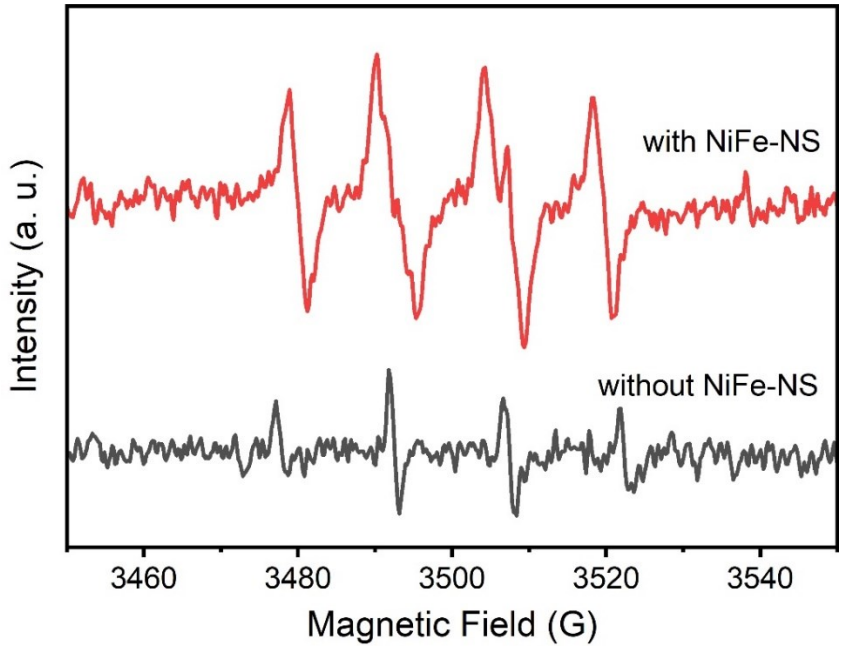

Figure S17. DMPO spin-trapping EPR spectra recorded for DMPO-·OH (0.10 M DMPO, 12.5 μL 30 wt% H_2O_2, 0.5 mL H_2O, λ>400 nm).

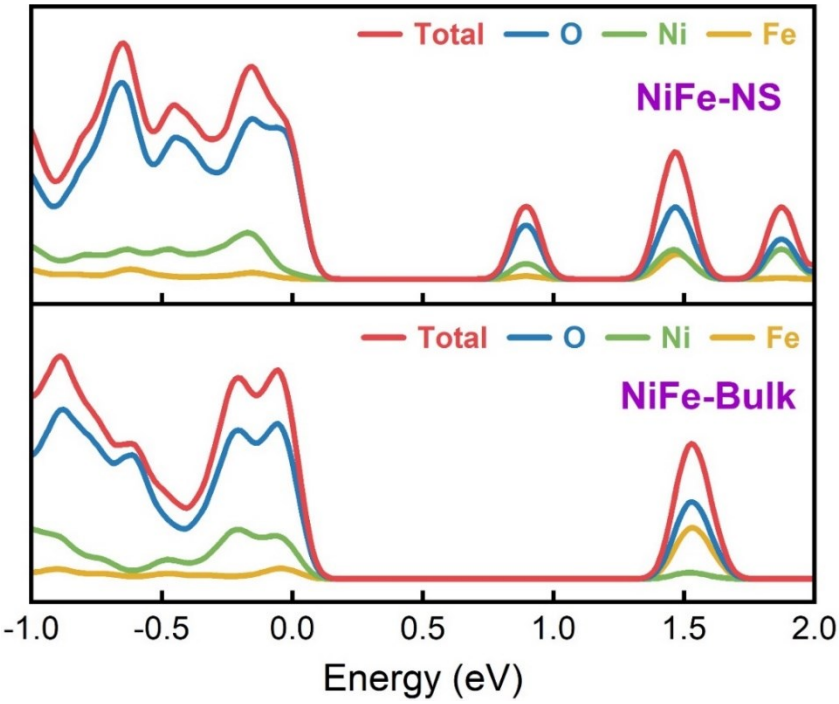

Figure S18. Calculated DOS of NiFe-NS and NiFe-Bulk.

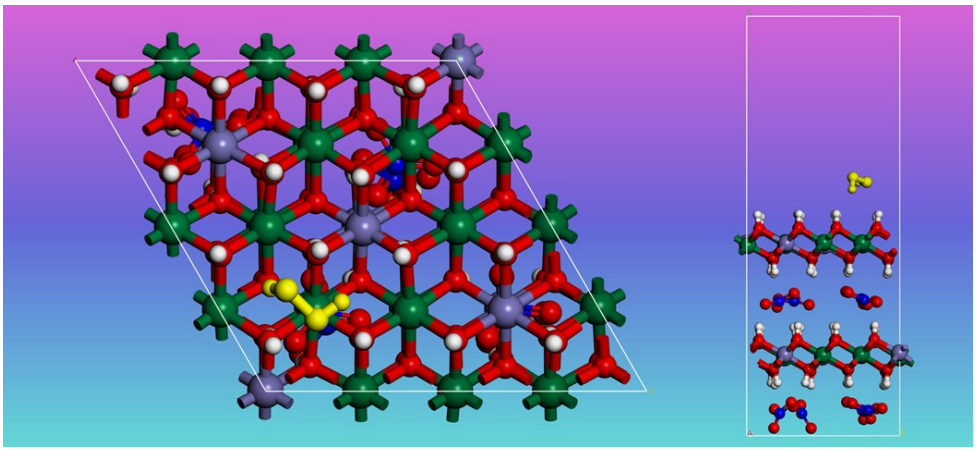

Figure S19. Illustration of the optimized geometry of H_2O_2 on the surface of NiFe-Bulk (H_2O_2 molecule is highlighted as yellow).

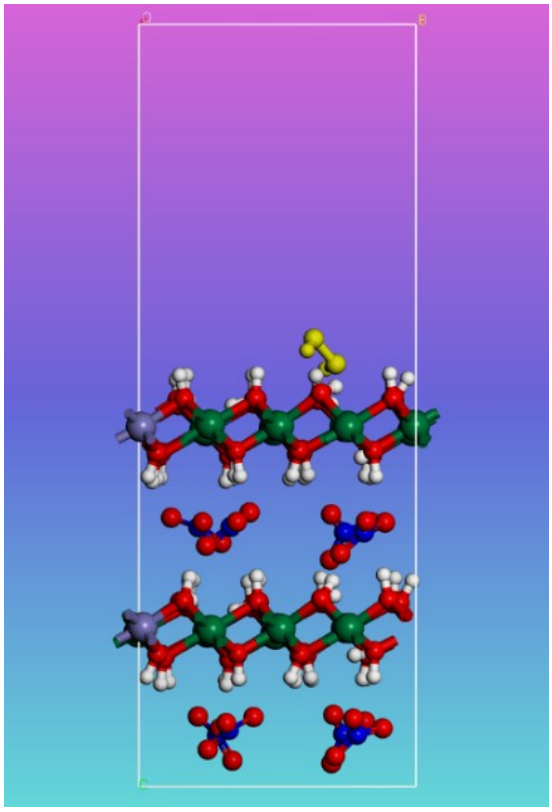

Figure S20. Illustration of the optimized geometry of H_2O_2 on NiFe-NS (H_2O_2 molecule is highlighted).

Reference

1. W. S. Putro, T. Kojima, T. Hara, N. Ichikuni and S. Shimazu, *Catal. Sci. Technol.,* 2018, **8**, 3010-3014.
2. P. Gholami, L. Dinpazhoh, A. Khataee, A. Hassani and A. Bhatnagar, *J. Hazard. Mater.*, 2020, **381**, 120742.
3. R. Mészáros, S. B. Ötvös, Z. Kónya, Á. Kukovecz, P. Sipos, F. Fülöp and I. Pálinkó, *React. Kinet. Mech. Catal.*, 2017, **121**, 345-351.
4. M. Laipan, H. Fu, R. Zhu, L. Sun, J. Zhu and H. He, *Sci. Rep.*, 2017, **7**, 7277.
5. Z. He, J. Wu, B. Gao and H. He, *ACS Appl. Mater. Interfaces*, 2015, **7**, 2424-2432.
6. R. Yang, G. Li and C. Hu, *Catal. Sci. Technol.*, 2015, **5**, 2486-2495.
7. H. Zhang, C. Tang, Y. Lv, C. Sun, F. Gao, L. Dong and Y. Chen, *J. Colloid Interface Sci.,* 2012, **380**, 16-24.
8. S. Yang, G. Liang, A. Gu and H. Mao, *Appl. Surf. Sci.*, 2013, **285**, 721-726.
9. F. Adam, J. Andas and I. A. Rahman, *Chem. Eng. J.*, 2010, **165**, 658-667.
10. F. Adam, J.-T. Wong and E.-P. Ng, *Chem. Eng. J.*, 2013, **214**, 63-67.
11. S. Samanta and R. Srivastava, *Appl. Catal. B Environ.*, 2017, **218**, 621-636.
12. C. Shan, Z. Li, L. Wang, X. Su, F. Shi and J. Hu, *Catal. Commun.*, 2017, **101**, 116-119.
13. H. Shi, T. Zhang, B. Li, X. Wang, M. He and M. Qiu, *Catal. Commun.*, 2011, **12**, 1022-1026.
14. H. Shi, T. Zhang, T. An, B. Li and X. Wang, *Curr. Org. Chem.*, 2012, **16**, 3002-3007.